

## Interannual variability in phytoplankton biomass and species composition in northern Marguerite Bay (West Antarctic Peninsula) is governed by both winter sea ice cover and summer stratification

P. D. Rozema,<sup>1\*</sup> H. J. Venables,<sup>2</sup> W. H. van de Poll,<sup>1</sup> A. Clarke,<sup>2</sup> M. P. Meredith,<sup>2</sup> A. G. J. Buma<sup>1,3</sup>

<sup>1</sup>Department of Ocean Ecosystems, Energy and Sustainability Research Institute Groningen, University of Groningen, Groningen, the Netherlands

<sup>2</sup>British Antarctic Survey, High Cross, Madingley Road, Cambridge, United Kingdom

<sup>3</sup>Arctic Centre, University of Groningen, Groningen, the Netherlands

### Abstract

The rapid warming of the West Antarctic Peninsula region has led to reduced sea ice cover and enhanced glacial melt water input. This has potential implications for marine ecosystems, notably phytoplankton growth, biomass, and composition. Fifteen years (1997–2012) of year-round size fractionated chlorophyll *a* (Chl *a*), phytoplankton pigment fingerprinting and environmental data were analyzed to identify the relationship between sea ice cover, water column stability and phytoplankton dynamics in northern Marguerite Bay, Antarctica. Over the investigated period, both summer (December–February) and winter biomass declined significantly, 38.5% and 33.3% respectively. Winter phytoplankton biomass was low ( $< 0.25 \mu\text{g Chl } a \text{ L}^{-1}$ ) and consisted on average of 69% diatoms, 5% cryptophytes, and 20% haptophytes. Summers following winters with low ( $< 65$  days) sea ice cover were characterized by decreased stratification strength and relatively low (median  $< 4.4 \mu\text{g Chl } a \text{ L}^{-1}$ ) phytoplankton biomass, as compared to summers preceded by high winter sea ice cover. In addition, the summertime microphytoplankton ( $> 20 \mu\text{m}$ ) fraction was strongly decreased in the low biomass years, from 92% to 39%, coinciding with a smaller diatom fraction in favor of nanophytoplankton ( $< 20 \mu\text{m}$ ), represented by cryptophytes and haptophytes. In contrast, diatoms dominated ( $> 95\%$ ) during summers with average-to-high biomass. We advance a conceptual model whereby low winter sea ice cover leads to low phytoplankton biomass and enhanced proportions of nanophytoplankton, when this coincides with reduced stratification during summer. These changes are likely to have a strong effect on the entire Antarctic marine food web, including krill biomass, and distribution.

Climate change strongly affects the physical environment in many different regions of our planet. One of the regions most profoundly affected is the West Antarctic Peninsula (WAP). Annual mean air temperatures over the WAP have increased by 2–3°C over the past 50 years (Turner et al. 2005), whilst summertime sea surface temperatures increased by more than 1°C (Meredith and King 2005). The increase in temperatures in the WAP region is associated with a

shortening of the sea ice season and an increase in glacial ice discharge (Depoorter et al. 2013; Rignot et al. 2013). These large-scale changes are strongly affecting the physical and chemical properties of the water column and may thereby affect marine food webs as well (Constable et al. 2014). Pronounced changes in sea ice cover have been observed in the coastal WAP region (Vaughan et al. 2003; Meredith and King 2005; Harangozo 2006). Sea ice duration has decreased by almost 90 days in the 1979–2004 period. This decrease contrasts with the general trend of modestly increasing sea ice extent around Antarctica as a whole, which is driven in particular by major advances in the Ross Sea with much slower rates of change elsewhere (Stammerjohn et al. 2008b; Montes-Hugo et al. 2009). The reduction of sea ice at the WAP is primarily due to a strong trend towards a later autumn advance and a somewhat weaker trend towards an earlier spring retreat (Stammerjohn et al. 2008b). As a

\*Correspondence: P.D.Rozema@rug.nl

Additional Supporting Information may be found in the online version of this article.

This is an open access article under the terms of the Creative Commons Attribution License, which permits use, distribution and reproduction in any medium, provided the original work is properly cited.

consequence, mean annual sea ice cover in the WAP area has decreased by 40% over a 26-year period (Smith and Stammerjohn 2001).

Another effect of warming of the WAP region is the enhanced influx of glacial melt water during summer, due to accelerated glacial retreat (Cook et al. 2005). Marguerite Bay, a major embayment in the central part of the WAP, is surrounded by retreating glaciers and is strongly influenced by the changing sea ice dynamics (Cook et al. 2005; Montes-Hugo et al. 2009; Meredith et al. 2010). In Marguerite Bay, decreased ice cover has been linked to a deepening of the winter mixed layer (Venables et al. 2013). Occasional strong winds during summer can cause well-described mixing events and can lead to a relatively short-term change in mixed layer depth (MLD). However, recent findings from northern Marguerite Bay have associated decreased winter ice cover to reduced stratification during the following spring and summer (Venables et al. 2013). Strong winds and decreased buoyancy during winter can mix the water column to greater depths during periods of low ice cover. These waters then require more buoyancy to be stabilized to the same level during the subsequent spring and summer, thus potentially leading to persistently weaker stratification. Additionally, the production of less sea ice in winter can lead to smaller volumes of ice being available to melt the following spring and summer, thus reducing the potential buoyancy input to restratify the upper ocean.

Seasonal dynamics of phytoplankton are strongly regulated by the timing of sea ice retreat. Austral spring marks the beginning of significant phytoplankton growth after a period of near darkness during winter, in particular when coinciding with water column stabilization caused by warming or freshening due to melt water input from melting sea ice or glaciers. Stabilization of the water column leads to a decreased MLD, thus light conditions become favorable for phytoplankton growth and bloom formation (Sverdrup 1953). Deep mixing due to periods of strong wind or convection can reduce the light available for photosynthesis. Even though the timing of the onset of the phytoplankton bloom may not change with a deeper mixed layer (Venables et al. 2013), it can influence the phytoplankton community through total biomass and/or species composition.

In coastal Antarctic waters, phytoplankton spring blooms under stratified conditions typically consist of large ( $> 20 \mu\text{m}$ ) diatoms that are favored under relatively high irradiance conditions (Arrigo et al. 1999; Clarke et al. 2008; van de Poll et al. 2009; Annett et al. 2010). In well-mixed waters around Antarctica, dominance can shift to the common and widespread haptophyte *Phaeocystis antarctica* (Arrigo et al. 1999; Alderkamp et al. 2012b). The periods of dominance by nanophytoplankton other than *Phaeocystis*, mainly cryptophytes, seem to be associated with glacial melt water stratification during summer, decreased nutrient stocks after spring and summer blooms (Buma et al. 1992; Moline et al. 2004;

Kozłowski et al. 2011; Mendes et al. 2012), and low irradiance conditions during winter (Clarke et al. 2008). Other phytoplankton groups frequently observed, although often in relative low and constant absolute abundances, are chlorophytes, dinoflagellates and prasinophytes (Kozłowski et al. 2011). A negative trend in microphytoplankton biomass in the northern WAP region, as observed by satellite, was linked previously to a deeper mixed layer and decreased ice cover (Montes-Hugo et al. 2009). This trend is opposite to that observed along the southern most sections of the WAP, where microphytoplankton is increasing due to the opening up of areas previously covered by sea ice.

Shifts within the size class distribution of phytoplankton have the potential to alter the Southern Ocean food web drastically (Atkinson et al. 2004). Krill abundance, pivotal within this ecosystem, has shown a strong dependence on sea ice-associated phytoplankton biomass (Saba et al. 2014). Declining phytoplankton stocks, mainly the microphytoplankton that is the preferred food for krill, are causing decreased success in krill recruitment north of Anvers Island (northern WAP; Montes-Hugo et al. 2009; Saba et al. 2014). So far, krill stocks in January-February in the southern section of the WAP appear to be stable (Steinberg et al. 2015). But juvenile krill depends on sea ice algae during winter, and are therefore affected negatively by the disappearance of sea ice (Trivelpiece et al. 2011; Flores et al. 2012; Reiss et al. 2015). As a result, future krill stocks in the southern WAP could be affected. Thus, the already observed changes within the Southern Ocean food web could be propagated to the region of the WAP (Schofield et al. 2010; Constable et al. 2014).

In northern Marguerite Bay, phytoplankton biomass estimated by remote sensing has been declining recently in comparison to the 1978–1986 period (Montes-Hugo et al. 2009). A clear example of reduced sea ice cover is the winter of 1998, which led to deeper mixing that persisted through to the subsequent summer (Meredith et al. 2004; Stammerjohn et al. 2008a) and which was associated with a decrease in phytoplankton biomass (Clarke et al. 2008; Venables et al. 2013). While data describing phytoplankton species composition in Marguerite Bay are sparse, available data are comparable to those of the larger WAP region (Garibotti et al. 2005; Kozłowski et al. 2011), showing the dominance of microphytoplankton ( $> 20 \mu\text{m}$ ; Clarke et al. 2008). Diatoms dominate this size class, however there is large variability with respect to species composition (Garibotti et al. 2003, 2005; Annett et al. 2010; Piquet et al. 2011). No long-term year-round phytoplankton studies are available for the area. Data from the adjacent Palmer Long-Term Ecological Research (LTER) grid spans  $\sim 20$  years, however these are limited to the summer period (Kozłowski et al. 2011).

In the present study we analyzed phytoplankton dynamics in northern Marguerite Bay as a function of winter sea ice conditions and summer stratification, obtained from a

long-term ocean monitoring site adjacent to the British Antarctic Survey's Rothera Research Station. Phytoplankton dynamics were elucidated using 15 years of year-round size-fractionated chlorophyll *a* (Chl *a*) supplemented with 7 years of pigment fingerprinting (HPLC-CHEMTAX). We aim to propose a conceptual model that allows us to understand the large variability in observed phytoplankton biomass. The almost unique year-round nature of this dataset is valuable in explaining some of these large variations in phytoplankton biomass and composition, not only related to summer stratification, but also to winter ice dynamics.

### Materials and methods

Samples for the monitoring of biological and physical oceanographic variables were collected at the RaTS site (Rothera Oceanographic and Biological Time Series; 67.570°S 68.225°W, details in Clarke et al. (2008) and Venables et al. (2013)) located near Rothera Research Station on the WAP (Fig. 1). The monitoring site is situated in Ryder Bay, which is part of the northern Marguerite Bay region. Venables and Meredith (2014) showed that the RaTS location in Ryder Bay is representative of the broader physical environment across northern Marguerite Bay. The distance between the nearest shore and the RaTS site is ~2 km, and the maximum depth is ~520 m. Data were collected between April 1997 and October 2012. Desired sampling frequency during the summer was twice per week, and once per week in winter. Samples were collected by small boat, unless sea ice precluded accessing of the sampling site. Under these conditions, an alternative site (67.581°S 68.156°W) was used in ~300 m of water and located approximately the same distance from the shore. During periods of heavy land-fast-ice, samples were collected through a hole cut in the ice. A gap in the series of measurements was defined if no samples were collected for a period of 30 days or longer (Fig. 2b).

Depth profiles of temperature, conductivity, pressure and fluorescence were obtained using a conductivity-temperature-depth (CTD) instrument. Initially, a Chelsea Instruments Aquapak CTD and fluorometer was used, with a maximum depth rating of 200 m. This instrument was replaced in January 2003 by two CTDs, one SeaBird 19+ CTD and a SeaBird 19 CTD both with a WetLabs in-line fluorometer enabling full depth (500 m) profiles. Variables measured using the CTD were averaging into 1 m bins. Calibration of the CTDs between years and with the Palmer LTER program measurements are discussed in Venables et al. (2013).

Phytoplankton samples were collected at 15 m depth using 2 to 10 L Niskin bottles. This fixed depth was used since it is the depth of the fluorescence maximum, and was reasonably representative of the total biomass in the water column (Clarke et al. 2008). While in transit from the sampling location, samples were stored in insulating blankets and/or boxes to prevent freezing.

Sea ice cover and type were characterized as described in Venables et al. (2013). In short, daily observations were made from an observation tower and considered sea ice conditions in three bays around the research station. We define fast-ice cover as days with  $\geq 80\%$  coverage of the area by fast-ice. Even though multiple observers throughout the years can introduce internal heterogeneity in the series due to the observations' subjective nature, such errors were still smaller than the large interannual variability in physical changes within the region (Venables and Meredith 2014).

MLD was defined as the depth at which the difference between the observed density and surface (1 m) density was  $\geq 0.05 \text{ kg m}^{-3}$ . Stratification was quantified by calculating the potential energy required to homogenize the water column from the surface to 30 m. This metric of stratification is the negative of the potential energy anomaly, in  $\text{J m}^{-2}$  (Simpson et al. 1978).

The onset of summer melt was defined as the Julian day on which salinity at 15 m was 0.05 lower on the practical salinity scale than the highest salinity observed during the previous winter at 15 m. Also, if salinity at 15 m increased by  $> 0.025$  on the practical salinity scale during spring, generally as a result of wind mixing, the day of summer melt was defined after this event. Our rationale for using these measurements as a possible proxy for median summer biomass was that spring conditions were influenced by the previous winter conditions (sea ice cover, date of retreat, MLD, etc.) as well as current spring conditions (temperature, melt, wind speed, etc.). This could be reflected by the time point during spring when stratification started. We therefore chose to investigate the relationship between the Julian day showing the first significant decline in salinity (15 m) and subsequent median summer biomass. Determination of such a date proved challenging as data collection during spring was frequently hindered by unfavorable sea ice conditions. No data were collected for 1.5 months due to sea ice conditions during the spring 2006–2007 and therefore this spring period was excluded from the analysis.

For size-fractionated Chl *a* analysis, triplicate samples (250 – 2000 mL each) were filtered through sequential 47 mm filters into microphytoplankton ( $> 20 \mu\text{m}$ , Nylon mesh filter), large nanophytoplankton (20–5  $\mu\text{m}$ , membrane filter), small nanophytoplankton (5–2  $\mu\text{m}$ , membrane filter) and picophytoplankton (2–0.2  $\mu\text{m}$ , membrane filter) fractions. Filtrations were conducted in the dark and at 4°C, and were started immediately after return to the laboratory (within 60 minutes after sampling). Chl *a* analyses were conducted as described in Clarke et al. (2008) and based on Wood (1985); in short, pigment extractions were performed overnight at 4°C in chloroform/methanol (2:1 v/v) and Chl *a* was determined before and after the addition of 0.1 N HCl using a fluorimeter (AU-10, Turner). Total Chl *a* concentrations were calculated by summing the four size fractions.

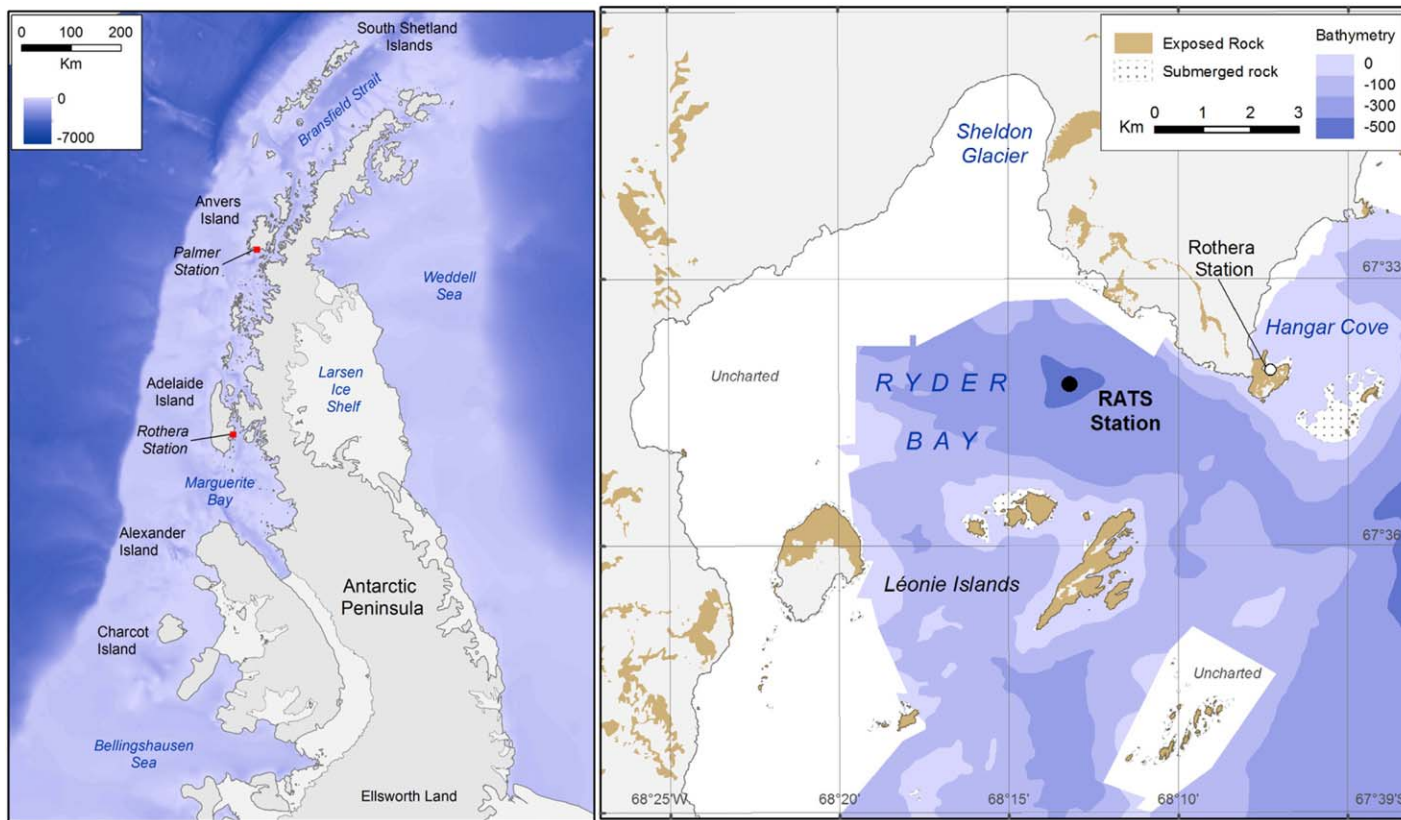


**Fig. 1.** Left a map showing the West-Antarctic Peninsula marked with both the Rothera and Palmer stations. Secondly, a close up of the vicinity of Rothera Research Station with the long-term RaTS site is shown on the right.

Collection of samples for pigment analysis by high-pressure liquid chromatography (HPLC) on GF/F (47 mm, Whatman) started in October 2005, and was conducted by filtering 1 L of seawater using a moderate vacuum. The results presented here are based on 268 GF/F filters collected from September 2005 until November 2012. Filtering started immediately after the return to the laboratory, and was conducted under low light. Filters were snap frozen in liquid nitrogen and stored at  $-80^{\circ}\text{C}$  until further processing. Samples for pigment analysis using HPLC were not taken or analyzed if no liquid nitrogen was available.

Prior to extraction, the filters were freeze dried for 48 h in the dark. To extract the pigments, the filters were incubated in 90% acetone (v/v) at  $4^{\circ}\text{C}$  in the dark for 48 h (van Leeuwe et al. 2006). Pigments were separated on a Waters 2695 HPLC system using a Zorbax Eclipse XDB-C8 column ( $3.5\ \mu\text{m}$  particle size) as described by Van Heukelem and Thomas (2001) and modified by (Perl 2009). Diode array spectroscopy type 996 (Waters, US) and retention times were used for manual pigment identification and quantification. Calibration of the system was performed against standards (DHI LAB PRODUCTS) for chlorophyll c3, chlorophyll c2,

peridinin, 19'-butanoyloxyfucoxanthin, fucoxanthin, neoxanthin, prasinoxanthin, 19'-hexanoyloxyfucoxanthin, alloxanthin, lutein, chlorophyll b and chlorophyll a1.

Calculation of the abundance of various phytoplankton groups based on their pigment signatures was conducted using CHEMTAX v1.95 (Mackey et al. 1996). This program uses a factor analysis and steepest descent algorithm to find the best fit based on initial pigment ratios. Eight different phytoplankton classes were chosen to be representative of the marine Antarctic ecosystem (Wright et al. 2009, 2010; Higgins et al. 2012); prasinophytes, chlorophytes, dinoflagellates, cryptophytes, two types of haptophytes and two types of diatoms. Microscopic observations from two summer seasons at the RaTS station were taken into account when determining which classes to include in our CHEMTAX matrix (Annett et al. 2010). We distinguished between two haptophyte groups because the dominant haptophyte *Phaeocystis antarctica* can show high variability in ratios of 19-butanoyloxyfucoxanthin, fucoxanthin and 19-hexanoyloxyfucoxanthin to Chl a ratios under varying light conditions and iron concentrations (reviewed in van Leeuwe et al. (2014)). Also, two types of diatoms (Diatoms 1 and 2) were included. Diatoms 2 include species such as *Pseudonitzschia sp.* and *Proboscia sp.*, often



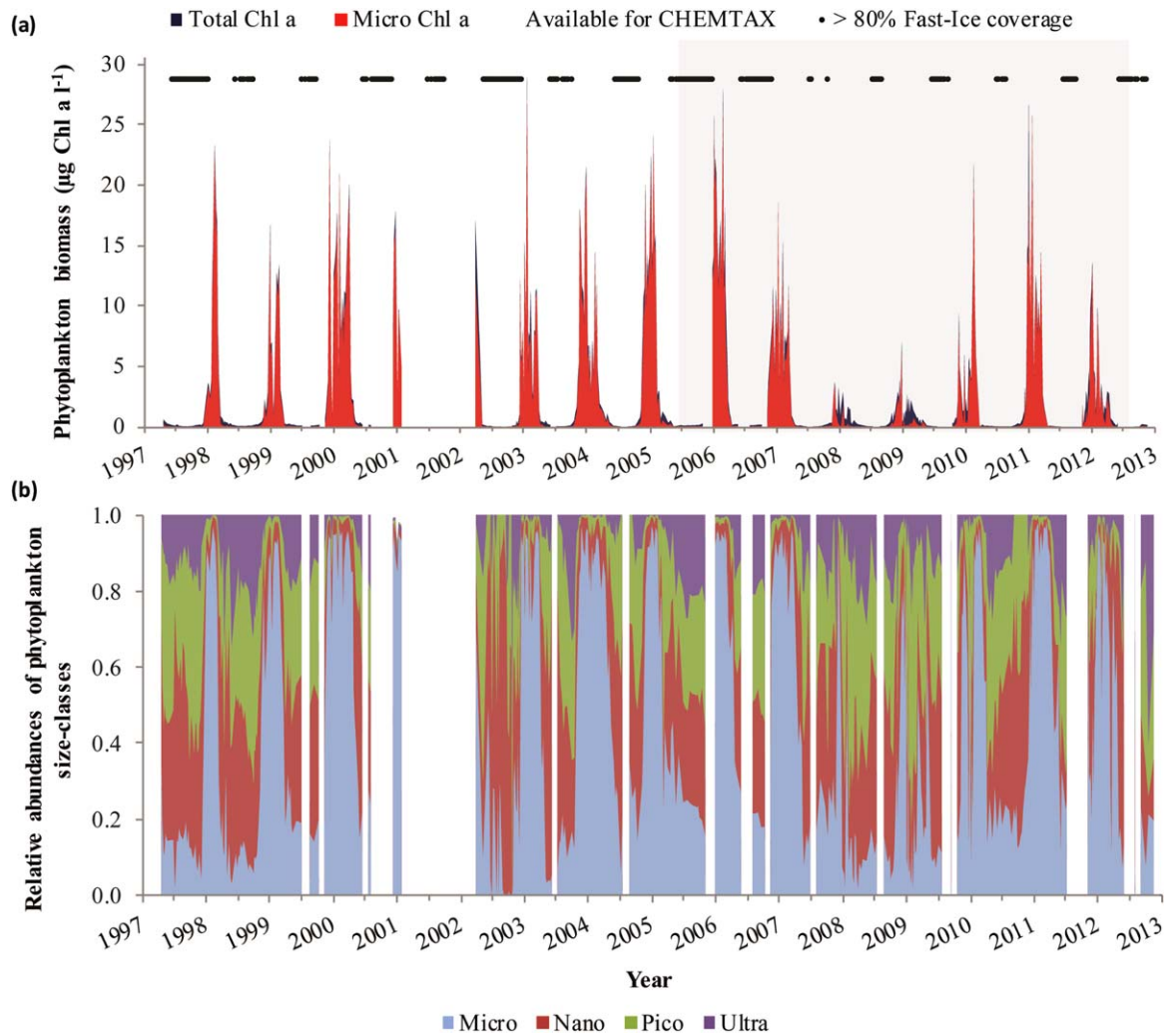


**Fig. 2.** (a) Time series of total and microphytoplankton biomass relative (both in Chlorophyll *a*) at the RaTS site. Years within the grey area were available for pigment analysis by HPLC. (b) Relative abundance of microphytoplankton, nanophytoplankton, picophytoplankton, and ultraphytoplankton, based on size-fractionated chlorophyll *a*. Gaps within both time series mark periods where the RaTS site was not sampled for 30 days or more.

observed in sea ice ecosystems and at RaTS, and contain chlorophyll *c3* whereas most other diatom species (Diatoms 1) do not (Annett et al. 2010). The initial ratios for the different phytoplankton classes were constructed using published results from various sources describing pigmentation of Antarctic phytoplankton (Supporting Information Table S1).

Pigment concentration data were sorted in eight bins; seven bins for the seven different summer seasons (2005–2012) and one bin for all winter samples combined as these samples were taken less frequently. Summer and winter bins were defined using a cluster analysis on all pigment concentrations. City-block distances were calculated and samples clustered according to Ward's method (Latasa et al. 2010). Samples with very low biomass clustered together. The limit of low biomass ( $< 0.25 \mu\text{g L}^{-1}$  Chl *a*) was found to be distinctive between the summer and winter samples. Thus, samples with low biomass were considered a winter sample if no increase in biomass

occurred within 14 days after the sample was taken. The initial ratio's matrix was separately optimized for the summer and winter bins. Using two classes for haptophytes and diatoms greatly improved the residual mean square error (RMSE). Exclusion of chlorophyll *c2*, neoxanthin and prasinoxanthin in the winter bin resulted in a strong decrease in RMSE during the initial exploratory CHEMTAX analyses (Supporting Information Table S1). Low values for the RMSE for the 8 summer bins resulted in the inclusion of all 12 pigments for the summer samples. As the algorithm of CHEMTAX is prone to being stuck at local minima, we ran CHEMTAX 60 times (reviewed in Kozłowski et al. (2011)). The first run used the initial ratio matrix as taken from the literature while the ratios for the subsequent runs were varied randomly by  $\pm 35\%$  of the initial ratios (Wright et al. 2009). Chl *a* was always defined as 1. After the 60 runs, the run with the lowest RMSE per bin was checked to ensure that the final ratios were ecologically

realistic. If so, then those results were considered the best possible result. Final ratios are included in Supporting Information Table S1. Settings for the CHEMTAX program were as described in Kozłowski et al. (2011) with all the elements varied.

Classification of winter samples in the size-fractionated Chl *a* time series, as needed for statistical purposes, was as used for defining the winter bin for the CHEMTAX analysis (see above). We refrained from using a fixed period as sampling effort during winter was variable due to inaccessibility of the site. Summer samples were defined as all the samples collected in December, January, and February. These classifications were employed to discuss long term trends in the relative abundance of phytoplankton size fractions and total Chl *a* during summer and winter using linear regressions.

To differentiate between the different summers and winter relative phytoplankton species composition we used a non-parametric multivariate analysis of variance (NPMANOVA) with the Bray-Curtis distance measure and 9999 permutations. This was supplemented by post-hoc pairwise Hotelling's tests if the initial analysis was found significant (Anderson 2001) and corrected with a Bonferroni correction (alpha 0.05) to avoid type 1 errors (Holm 1979). Further exploration of the relative phytoplankton composition and its interannual variability was tested by using a Non-metric multidimensional scaling (NMDS). The NMDS scores were rotated using a Principal Component Analysis (PCA) to maximize the case scores along the two axes. The PCA shows how the various phytoplankton groups characterize the different summers and which summers were similar to one another.

To understand the relationship between winter MLD, duration of fast-ice cover and summer stratification strength, we used second PCA-rotation of NMDS scores with Euclidian distances. Before the NMDS, the data were log-transformed and their means subtracted to correct for differences in the scale of the variables. A minimum spanning tree of the initial NMDS scores depicts how the years were oriented within the initial three-dimensional space of the NMDS. The exclusion of biological parameters allowed us to test if the water column properties differed significantly between the years. Stress of the initial NMDS, as calculated by Shepard's plots, was  $\sim 0.05$ .

A correlation table was used to assess linear relationships between winter MLD, duration of fast-ice cover, median summer Chl *a* and summer stratification strength as our phytoplankton data do not cover the full duration of the time series (Venables et al. 2013). The correlation table was expanded with the median relative abundances of the different phytoplankton groups. Spearman's rank coefficients were calculated to test for correlations both between the environmental parameters (winter MLD, duration of fast-ice cover, median summer Chl *a* and summer stratification strength) and phytoplankton abundance and between the various abundances of the phytoplankton groups. We opted for a rank-based approach due to the non-linear nature of

phytoplankton responses to changing environmental conditions. The correlations were assumed significant if  $p \leq 0.05$ . For  $p \leq 0.1$  but  $> 0.05$ , correlations were reported as indicative of a possible relationship.

To classify the productivity of summers based on median summer Chl *a*, we used the results of the NMDS analyses. Grouping of years based on the winter MLD, duration of fast-ice cover and summer stratification strength was used to construct a conceptual model that predicts summer phytoplankton biomass and composition depending on winter and summer water column properties.

All statistical tests were conducted using PAST 2.17c (Hammer et al. 2001) except for the PCAs on the NMDS scores which were created using CANOCO 5.02.

## Results

Winter sea ice duration has been highly variable during the lifetime of the RaTS programme, 1997 to 2013 (Ducklow et al. 2013; Venables and Meredith 2014). Sea ice cover at the RaTS site was described in detail by Meredith et al. (2005, 2010) and updated in Venables and Meredith (2014). A greatly decreased presence of fast-ice (24–64 d) was observed during the winters of 1998, 2001, 2003, and 2007–2010 (Fig. 2a; Venables and Meredith, 2014). These reductions were linked to an increase in northerly winds driving the ice out of Ryder Bay (Meredith et al. 2010). In comparison to Adelaide Island, both Charcot Island and Anvers Island (Palmer Station; Fig. 1) displayed sea ice anomalies of the same sign but with a different scale (Ducklow et al. 2013). Anvers Island lies north of Adelaide Island, while Charcot is to the south, hence these locations are on a north-south climatic gradient along the WAP. When comparing the satellite-derived data to the direct observations of sea ice cover at Adelaide Island, good agreement is generally found (Ducklow et al. 2013; Venables and Meredith 2014).

An exception was the winter of 2003, when there was little fast-ice detected by satellite yet direct observations made at Rothera indicated 89 days of fast-ice coverage (Ducklow et al. 2013; Venables and Meredith 2014). Also, winter MLD during 2003 was relatively deep (75 m) suggesting an overestimation of sea ice cover in the direct observations. The average duration of fast-ice cover throughout the time-series was 76 days.

As a result of the high variability in winter sea ice presence, variation in winter MLD was also large. Mean winter MLD was  $\geq 75$  m during the years in which fast-ice coverage was low, with the exception of 2009 (Venables et al. 2013). In contrast, mean winter MLD averaged  $< 42$  m during the remaining years, with 2000 being the shallowest at only 16 m. Mean summer upper-ocean (30 m) stratification strength varied between  $462 \text{ J m}^{-2}$  (2010–2011) and  $124 \text{ J m}^{-2}$  (2007–2008). The results on winter MLD and summer stratification strength as used in the correlation analysis were updated from Venables et al. (2013).

During the full sequence of RaTS, variability in total phytoplankton biomass was high (Fig. 2a). Winter concentrations were low, averaging just  $0.061 \mu\text{g Chl } a \text{ L}^{-1}$  with stocks never exceeding  $0.194 \mu\text{g Chl } a \text{ L}^{-1}$ . Lowest winter biomass levels were found to be less than  $0.001 \mu\text{g L}^{-1}$ . Winter biomass levels decreased at a rate of  $0.023 \mu\text{g L}^{-1}$  per decade or 33.3% over the duration of the time series ( $df = 203$ ,  $p = 0.022$ ). The average contribution of microphytoplankton to total biomass during winter was 18.5%, and increased by 8.0% per decade ( $df = 203$ ,  $p < 0.001$ ) and varied between 0.00% and 64.9% (Fig. 2b), yet absolute microphytoplankton biomass remained unchanged. The three remaining smaller phytoplankton size classes decreased in absolute and relative abundance over the 1997–2012 winter periods.

Average summer (Dec–Feb) Chl *a* concentration was  $8.53 \mu\text{g L}^{-1}$  with frequent peaks of more than  $20 \mu\text{g L}^{-1}$ . The highest measured value was  $28.92 \mu\text{g L}^{-1}$  in January 2003. The summers of 2007–2008 and 2008–2009 were exceptional due to their extremely low maximum biomass maximum of  $6.96 \text{ Chl } a \mu\text{g L}^{-1}$ . Over the complete period (1997–2012), total summer (Dec–Feb) biomass decreased significantly by 38.5% or  $2.88 \mu\text{g Chl } a \text{ L}^{-1}$  per decade ( $df = 224$ ,  $p = 0.006$ ). On average, 75.0% of the summer Chl *a* stock was contained in microphytoplankton. This fraction was lower for 2007–2008 and 2008–2009, respectively, 32.2% and 30.9%.

Pigment fingerprinting followed by CHEMTAX analysis revealed that diatoms were the dominant group and relative abundances of this group rarely dropped beneath 50% (Fig. 3a). Median abundances of diatoms were 91.0% in summer and 71.4% for winter. Medians for the other phytoplankton groups during winter were 19.0% for haptophytes and 2.6% for cryptophytes with prasinophytes, dinoflagellates and chlorophytes remaining below 0.5%. Medians were used as they are less sensitive to extreme values, but this has the consequence that the values do not always add up to 100%. This illustrates that prasinophytes, chlorophytes and dinoflagellates were observed less frequently but could occasionally contribute to the winter community. In particular prasinophytes could be relatively abundant during winter with a mean of 4.9% yet a low median. Exceptionally high prasinophyte abundances were observed during the late summer of March 2006, when they dominated phytoplankton stocks with a relative abundance of 40.2–48.8%. On average, samples with an overall phytoplankton biomass higher than  $0.25 \mu\text{g Chl } a \text{ L}^{-1}$  were dominated by diatoms resulting in medians (mean in brackets) of: 1.6% (3.0%), 2.4% (7.3%) and 2.8% (6.8%) for prasinophytes, cryptophytes and haptophytes, respectively. Chlorophytes and dinoflagellates represented less than a median of 0.1% (average  $< 1.23\%$ ) of the summer biomass. The large difference between the medians and means for haptophytes and cryptophytes shows that these groups were more skewed in their variability. Also, dynamics within the summer season, which are lost by just means and/or medians, show that cryptophyte relative

abundance increased to 76.0% in January 2008, 58.9% in February 2009 and 23.2% in January 2010 (Fig. 3a). Haptophyte abundances reached 21.5% in February 2008, 40.3% in January 2009 and 29.9% in January 2010 (Fig. 3a).

As phytoplankton absolute abundance can be highly variable due to various environmental parameters, we choose to rely mainly on the relative abundances. A change in relative abundance does not necessarily mean that one group was increasing or decreasing in absolute numbers as relative abundance is highly dependent on the variability of the other phytoplankton groups. Thus, to validate any possible trend in cryptophyte and haptophyte absolute abundances with respect to relative abundance of diatoms we needed to validate our choice for the latter. When diatom relative abundance was low, cryptophyte absolute abundance was up to 11.8-fold higher than when diatoms were the dominating fraction ( $\geq 0.9$ ; Fig. 4a). Also, haptophyte absolute abundance was a maximum of 5.7-fold higher with a decreased relative abundance of diatoms (Fig. 4b).

Medians for the summer periods showed significant differences in group-specific abundances between years (Fig. 3b). In the years 2007–2008 and 2008–2009, both haptophytes and cryptophytes were relatively more abundant at the expense of diatoms. In addition, absolute diatom abundance was decreased while haptophytes and cryptophytes remained stable or showed higher abundances in comparison to periods of diatom dominance ( $> 90\%$ ). Following two low biomass summer seasons, 2009–2010 started with low biomass during the first half of summer, more haptophytes and cryptophytes and fewer diatoms in comparison to 2005–2006, 2006–2007, 2010–2011, and 2011–2012 (Fig. 3a). Yet, the 2009–2010 summer biomass levels reached average concentrations during the second half of summer, although median biomass remained low for the summer (Fig. 2a;  $4.42 \mu\text{g Chl } a \text{ L}^{-1}$ ). In contrast to these low biomass years, the summer seasons of 2005–2006, 2006–2007, 2010–2011, and 2011–2012 were highly similar with respect to relative abundances of the various phytoplankton groups.

Results from the NPMANOVA on the relative abundances of the phytoplankton groups revealed that the summers were not similar (pseudo- $F_{7, 187} = 14.46$ ,  $p < 0.0001$ ). First, pairwise comparisons (Table 1) show that the pooled winter samples were different from all the summer assemblages except for 2008–2009. Second, the summers of 2007–2008 and 2008–2009 were significantly different in comparison to the other years. The third low biomass summer, 2009–2010, was similar to all summers except 2010–2011. In addition, 2007–2008, 2008–2009, and 2009–2010 were considered equal to each other. Third, the summer seasons of 2005–2006, 2006–2007, 2010–2011, and 2011–2012 were found to be similar. The NMDS scores supported the results obtained from the NPMANOVA (Table 1, Fig. 5b). Here, the winter samples clustered close to the 2008–2009 samples which were related with high haptophyte abundance. In contrast,

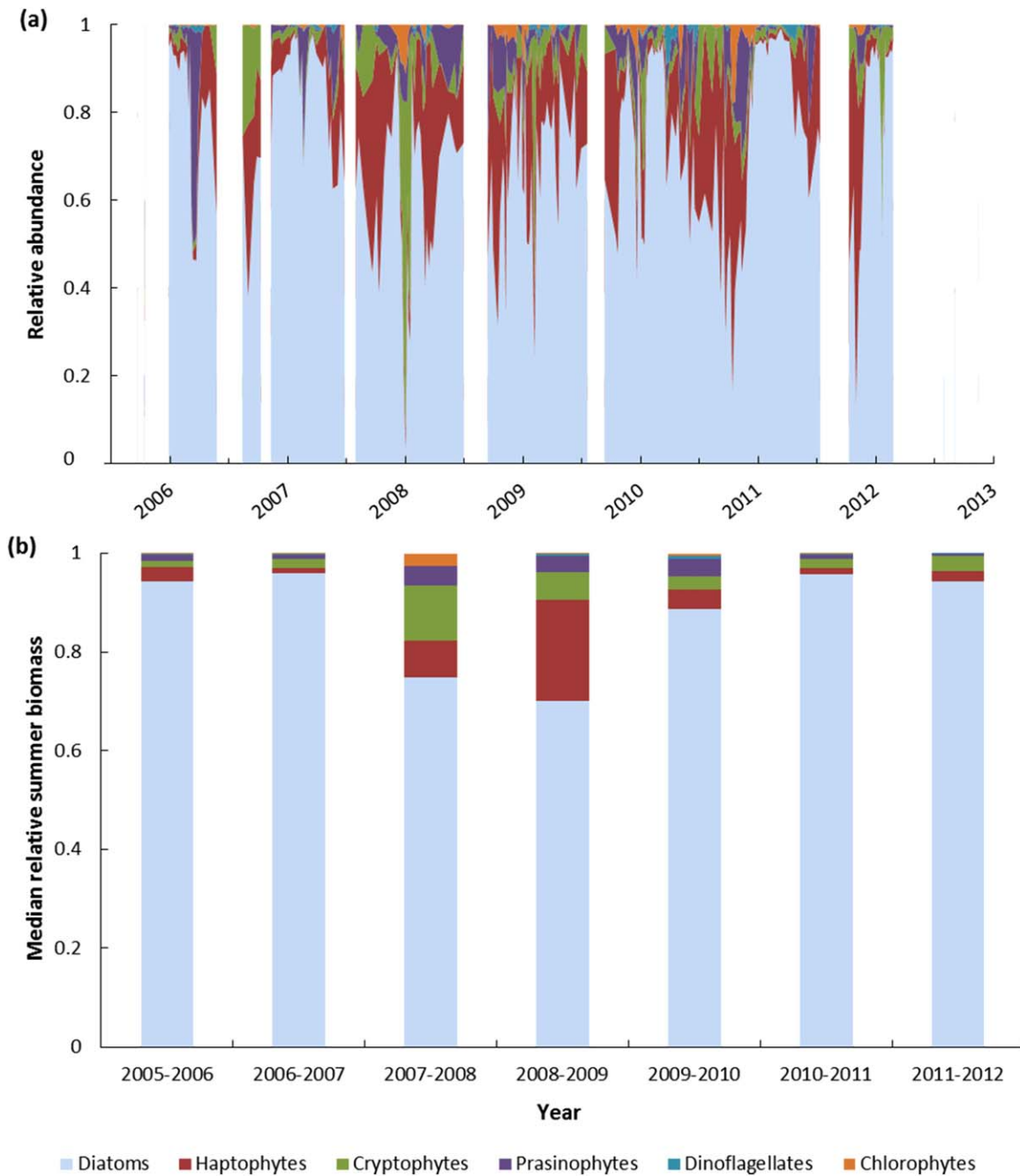


**Fig. 3.** (a) Relative abundance for the six most important phytoplankton groups based on CHEMTAX for the 2006–2012 period. Diatoms and haptophytes sub groups were combined after the analysis. Interruptions in the dataset indicate a gap in the dataset of more than 30 days. Year labels on the x-axis are at January (b) Median fractions per summer (December–February) of the CHEMTAX results. Data in both a and b were standardized to 100%.

2007–2008 was governed more by cryptophytes and overlapped only slightly with the winter samples. The results from the NPMANOVA for 2009–2010 were confirmed by the NMDS as this year overlapped with all other summers. Finally, 2005–2006, 2006–2007, 2010–2011, and 2011–2012 were clustered together indicating a highly similar phytoplankton community in terms of group-specific abundances.

The sudden increase of diatoms in the second half of January of 2010 could be related to melting sea ice from outside the bay. The summer of 2009–2010 was characterized (at 15 m) by a high average salinity (~33.4), an average sea water temperature and a very low contribution of glacial melt water (Figs. 9 and 10 in Meredith et al. 2013). However, after January 18th (Supporting Information Fig. S1a) there



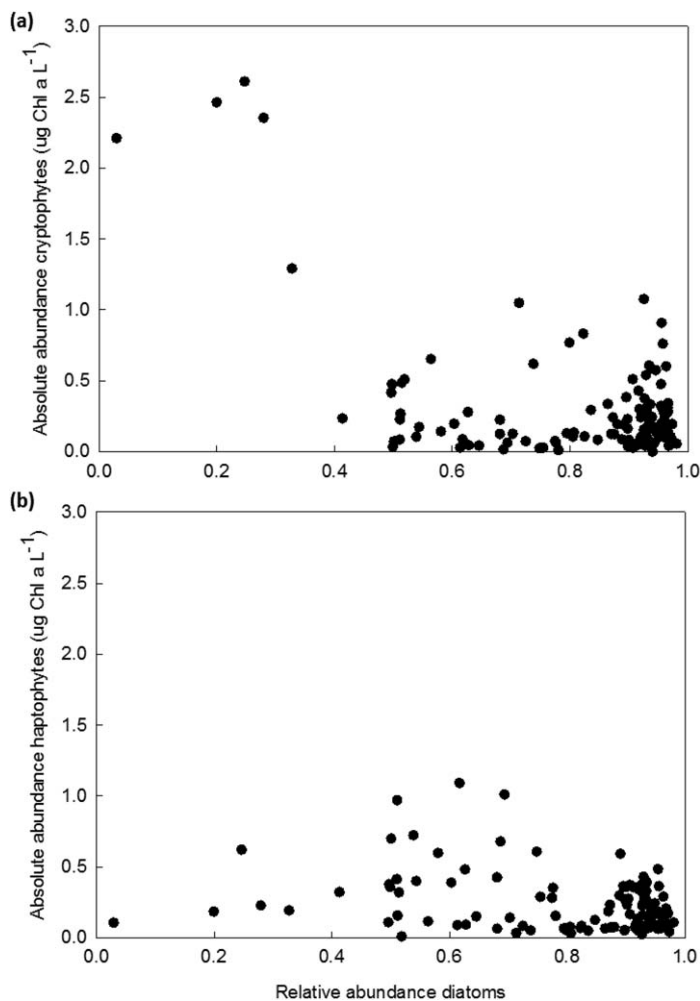


**Fig. 4.** Relative abundance of diatoms versus absolute abundance of (a) cryptophytes and (b) haptophytes. A decrease in the relative abundance of diatoms coincided with a large increase in absolute numbers of cryptophytes and haptophytes.

was a 0.5°C decrease in sea water temperature at 15 m and a small increase in salinity (~0.15). These changes coincide with a large increase (from 51.4% to 87.3%; Fig. 3a) in the relative contribution of diatoms. Also, after the sudden change on 18 Jan there was increased sea ice melt at the RaTS site which remained throughout February (Supporting Information Fig. S1b; Meredith et al. 2013).

To explore which physical characteristics could drive variability in phytoplankton composition, the medians of the relative summer abundances per group and year were correlated with previous winter mean MLD, summer chlorophyll median, number of fast-ice days in the previous winter and mean summer upper-ocean (top 30 m) stratification strength (Table 2). First, relative abundances of prasinophytes, haptophytes and cryptophytes were strongly negatively correlated with diatoms. This effect was strongest for cryptophytes and haptophytes. Second, weaker summer stratification was found to be directly

correlated with a lower relative abundance of diatoms. In contrast, abundances of prasinophytes, haptophytes and cryptophytes were positively influenced by a weakening of stratification in summer. Also, a weak positive relationship was found between the relative contribution of diatoms and total phytoplankton biomass (Table 2). Lower median summer Chl *a* was found to be associated with a larger proportion of cryptophytes. Finally, a significant and positive trend between winter MLD and cryptophyte abundance was observed.

Results of a PCA on NMDS scores for winter mean MLD, number of fast-ice days and mean summer upper-30 m stratification strength suggested a high similarity for these physical parameters between years with medium and low biomass (Fig. 5a). Also, the minimum spanning tree shows that the medium biomass years were closer to the low biomass years than to the high biomass years. Furthermore, 2010, a medium biomass year, was more similar to the low biomass years than to the other medium biomass years.

Even though both haptophytes and cryptophytes showed a negative relation with stratification strength they did not necessarily co-occur (Table 2). A further investigation of the summer MLD versus the relative abundance of both haptophytes and cryptophytes showed high abundances of cryptophytes during a shallow MLD (10–20 m), as could be deduced from the shape of the convex hull (Fig. 6a). No such relations (data not shown) were observed when relative abundances of haptophytes or cryptophytes were plotted against 0 or 15 m salinity, major nutrients (nitrogen, phosphate, silicate) or oxygen isotopes (indicative of melt water origin). Haptophytes do not seem to have a preferred MLD (Fig. 6b), occurring in similar relative abundances at various MLDs. Thus, even though the water column was, when averaged over the summer, unstable in comparison to medium/high biomass summers, short-term stratification events still occurred and seemed to have been associated with cryptophytes.

Median summer biomass appeared to be highly predictable ( $p = 0.002$ ;  $r^2 = 0.68$ ) when using the day when water column stabilization by fresh water input started to have a significant effect (Fig. 7). The difference between the earliest and latest start of the salinity decrease was 126 days (~4 months). This large difference in onset of the melt period resulted in a 16-fold difference in median biomass between the highest and lowest summer biomasses. The negative correlation suggests that an early onset of melt results in a highly productive summer or low productivity when melt is delayed. Spread of the observations for the high biomass summers is relatively large as sample collection was hindered more frequently by unfavorable sea ice conditions.

## Discussion

Our study showed large interannual variability in phytoplankton bloom magnitude and composition, related to winter sea ice cover and summer stratification strength. Microphytoplankton

**Table 1.** Post-Hoc testing after a NPMANOVA analysis on the relative species abundances from CHEMTAX for the summers (December–February) and the winter showed significant difference between the groups (pseudo- $F_{7, 187} = 14.46$ ,  $p < 0.0001$ ). The winter includes all winter samples of the 2005–2012 period pooled together as sample size was low. The table shows the Hotelling's  $p$  values after a Bonferroni correction for multiple testing ( $\alpha = 0.05$ ). Only values below 0.05 are shown and indicate significant differences between periods. The  $p$ -values are based on 9999 permutations.

		2005–2006	2006–2007	2007–2008	2008–2009	2009–2010	2010–2011	2012–2013	2005–2013
2005–2006	Dec–Feb	–							
2006–2007	Dec–Feb		–						
2007–2008	Dec–Feb	0.008	0.036	–					
2008–2009	Dec–Feb	0.003	0.003		–				
2009–2010	Dec–Feb					–			
2010–2011	Dec–Feb			0.003	0.003	0.020	–		
2011–2012	Dec–Feb			0.022	0.003			–	
2005–2012	Winter	0.003	0.003	0.003		0.031	0.003	0.003	–

(> 20  $\mu\text{m}$ ) dominated the summers between 1997 and 2013 except for 2007–2008 and 2008–2009 (Fig. 2a,b). Earlier observations by remote sensing linked an increase in MLD due to declining sea ice cover and an increased wind strength to a dominance of microphytoplankton > 20  $\mu\text{m}$  (Montes-Hugo et al. 2009). This is in line with our direct observations as microphytoplankton abundances in 2007–2008 and 2008–2009 were significantly decreased (Fig. 2b). The HPLC data at the RaTS station (7 out of the 15 years) showed that the observed decreasing trends in microphytoplankton were associated with a decline in diatoms (Annett et al. 2010). Our combination of size-fractionated Chl *a* with HPLC pigment fingerprinting appears to be a strong tool and can unravel the phytoplankton community responsible for the observed decrease in summer and winter phytoplankton biomass.

In contrast to summer, microphytoplankton did not contribute much to the winter and spring biomass (< 20%) while picophytoplankton (< 2  $\mu\text{m}$ ) represented > 48%. The 2007–2009 summers were more similar to the winter composition with regard to their size class distribution. These summers experienced steep increases of the microphytoplankton fraction when compared to the winter community. Yet, these increases lasted for a period significantly shorter than summers with a high biomass. Moreover, a summer with low biomass due to a decrease in (large) diatoms, does not necessarily imply a low microphytoplankton fraction. Colonies of *Phaeocystis antarctica* or large cryptophytes (> 20  $\mu\text{m}$ ) would be included in the microphytoplankton fraction. Both were observed frequently at the RaTS site by studying *in vivo* microscopy samples and revealed a high variability in cryptophyte cell sizes, ranging from < 10  $\mu\text{m}$  to > 20  $\mu\text{m}$  in cell length (A. Buma, unpublished results). Hence, the low biomass in 2009–2010 but average microphytoplankton fractions can explain the low relative abundance of diatoms as observed by CHEMTAX (Fig. 3a,b). This could also apply to 1997–1998, yet no HPLC data were available for this year.

Low light availability during winter due to deep mixing and the polar night limited phytoplankton growth and maintained a stable community with predominantly haptophytes (24%), cryptophytes (5%) and (small) diatoms (71%) (Figs. 2a, 3a, and 8). Differences in composition between winters were not tested due to a high variability in number of available samples per year. Pigment data suggest a dominance of diatoms during winter while size-fractionated Chl data suggested a low contribution of microphytoplankton, thus diatoms in winter were smaller than those in summer. This winter community would have experienced the first available light during spring and formed the base for the summer community. The seven years of HPLC data show the persistence of haptophytes and cryptophytes during spring (Fig. 3b). The spring phytoplankton assemblages in this study were all highly similar to those of winter.

Classical, well-described Antarctic diatom blooms propagate after spring when the water column has stabilized due to, e.g., glacial melt water input, surface warming and/or melt of fast-ice. However, a deeply mixed winter water column takes more buoyancy input (and, for a given rate of energy input, more time) to stabilize. This delay in stratification due to the lack of sea ice may have prevented the formation of classical diatom blooms in some years. Delayed onset of increased light availability caused the winter and spring communities to persist longer.

Our results show a highly similar and diatom-dominated composition between most summers (Table 1 and Fig. 5b). Diatom abundance and summer stratification were positively correlated (Table 2), in agreement with earlier observations at various Antarctic sites (Arrigo et al. 1999; Clarke et al. 2008; van de Poll et al. 2009; Annett et al. 2010; Piquet et al. 2011). However, we observed a larger presence of haptophytes (max. 40.3%) and/or cryptophytes (max. 76.0%) during summer periods with low biomass (2007–2010, Fig. 3a). Summers such as 2007–2008 and 2008–2009 showed that weak mean summer stratification, due to the absence of fast-

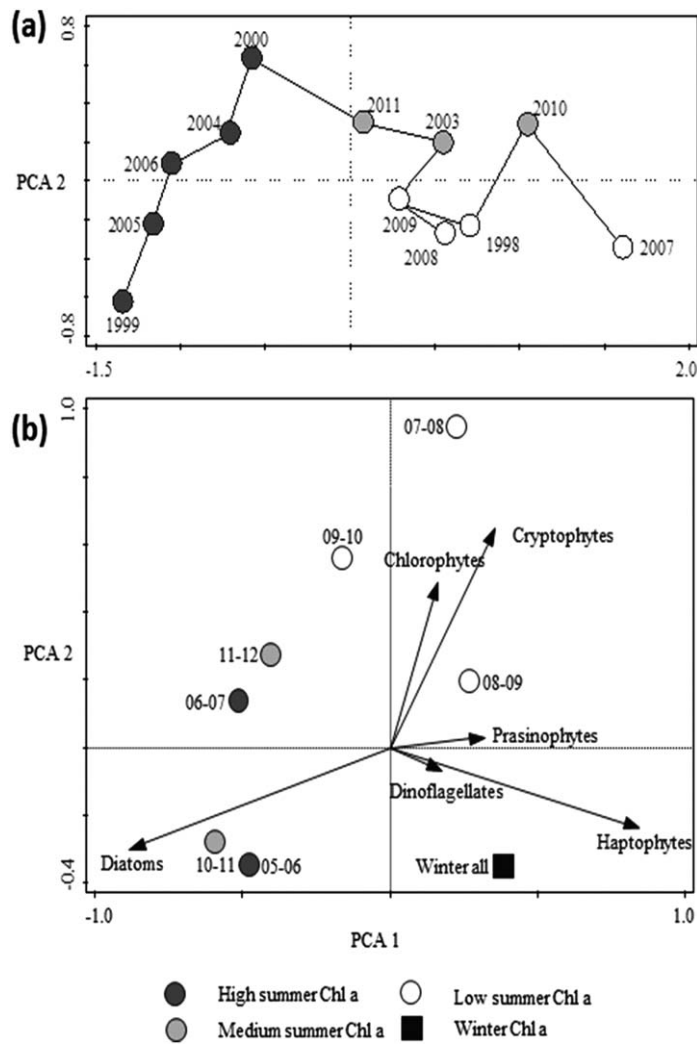


**Fig. 5.** Principal Component Analysis (PCA) on the scores of a Non-metric Multidimensional Scaling (NMDS) analysis. Data points are colored based on median summer biomass. The top graph (a) shows how the different years were related based on winter mean MLD, number of fast-ice days and mean summer upper-ocean (top 30 m) stratification strength. The lines connecting the years show the minimum spanning tree. The bottom graph (b) shows how strongly and to which season the relative abundance of different phytoplankton groups was related. Also, all pooled winter samples are plotted to compare the winter community to that of the different summers.

ice during winter, experience low diatom abundances. Although 2009–2010 shifted toward delayed diatom dominance, the median summer biomass remained low. The sudden change in water column conditions, an increase in salinity and decrease of the temperature, on 18 Jan 2010 could suggest lateral advection bringing in sea ice from elsewhere, as there was not much sea ice during winter (Fig. 2a, Supporting Information Fig. S1), altered the phytoplankton community. This is further supported by the exceptionally high contribution of sea ice melt observed during this

period (Supporting Information Fig. S1b; Meredith et al. 2013). This late increase of sea ice melt illustrates why 2009–2010 was placed in between two years belonging to two different classifications, namely 2007–2008 (low) and 2011–2012 (medium; Fig. 5b). In contrast, the two summers of 2007–2009 remained low in both biomass and diatom abundance. These two summers (and the first half of 2009–2010) suggest a persistence of the winter/spring community during years with weak summer stratification. This persistence was further strengthened by the lack of a significant difference between the summer of 2008–2009 and the pooled winter samples (Table 1). Not only did the relative abundances of cryptophytes and haptophytes increase when diatoms were less abundant, also absolute numbers increased (Fig. 4).

While both haptophytes and cryptophytes occasionally dominated, they did not necessarily co-occur (Table 2). Both groups were linked to unstable water column conditions, suggesting similar strategies for maintaining their presence (Table 2). Previous studies often associated *Phaeocystis* with well-mixed water columns in which average irradiance levels were low (Arrigo et al. 1999; Alderkamp et al. 2012b). Different strategies to cope with non-photochemical quenching following high irradiance exposure seems to be a major difference between diatoms and *Phaeocystis* (Kropuenske et al. 2009; Alderkamp et al. 2012a, 2013). Cryptophytes were often associated with low salinity and observed in the surface layer (Moline et al. 2004; Kozłowski et al. 2011; Mendes et al. 2013). Yet, our pigment data show a strong positive correlation with winter MLD and negative with summer stratification strength suggesting the opposite (Table 2). Also, cryptophytes were more abundant than haptophytes during periods in summer with a shallower MLD (Fig. 6). These two opposing observations suggest that surface stratification over an unstable and uniformly mixed water column favored cryptophytes. These conditions were possibly indicative of surface melt water stratification after periods of deep mixing. Apparently, cryptophytes cannot out-compete diatoms during years where water column stability is promoted earlier in the season. Prasinophytes were only present in high numbers during a small period at the end of the summer of 2005–2006. It is possible that this peak represents a small incursion of more open ocean waters, as prasinophytes were generally observed at depth at offshore stations (Kozłowski et al. 2011).

Limitation of phytoplankton growth by macronutrients during summer was unlikely due to generally high concentrations within the region, especially as low phytoplankton biomass was related to deeper (winter) mixing (Clarke et al. 2008). While micronutrients such as iron might limit phytoplankton growth, structural limitation is unlikely due to the coastal nature of the bay (Bown et al. in press; Alderkamp et al. 2012b; Annett et al. 2015). Temporary limitation of phytoplankton by low concentrations micronutrients might incidentally occur at RaTS although reported minimum

**Table 2.** Correlation table for the taxonomic groups were checked for correlation amongst themselves and with; mean winter mixed layer depth (MLD), Median summer Chlorophyll *a*, days of fast-ice cover and summer top 30m stratification strength. Significance values are (\*)  $p < 0.1$  show a trend but no significant correlation, \*\*  $p < 0.05$  and \*\*\*  $p < 0.001$ . Values and direction of the slope of the correlation (if  $p < 0.1$ ) are shown below the diagonal. Seven years of phytoplankton relative abundances were included (df = 5). Bray-Curtis distance and Spearman's rank coefficients were used for the comparisons between the phytoplankton groups and between the phytoplankton groups and physical parameters. Euclidian distances and linear correlations were used for comparisons of the physical parameters.

	Mean winter MLD (m)	Median chlorophyll <i>a</i> ( $\mu\text{g L}^{-1}$ )	Fast-ice cover (days)	Mean summer stratification top 30 m ( $\text{J m}^{-2}$ )	Prasinophytes	Chlorophytes	Dinoflagellates	Cryptophytes	Haptophytes	Diatoms
Mean winter MLD (m)	-	**	***	(*)						
Median chlorophyll <i>a</i> ( $\mu\text{g L}^{-1}$ )	-0.86	-	**	**						**
Fast-ice cover (days)	-0.95	0.83	-	(*)				(*)		**
Mean summer stratification top 30 m ( $\text{J m}^{-2}$ )	-0.71	0.84	0.67	-				***	**	**
Prasinophytes						(*)				
Chlorophytes					0.68	-				
Dinoflagellates										-
Cryptophytes	0.79	-0.96	-0.68	-0.93					(*)	**
Haptophytes		-0.75	-0.86	-0.86	0.75			0.68	-	**
Diatoms		0.86	0.82	0.82				-0.82	-0.82	-

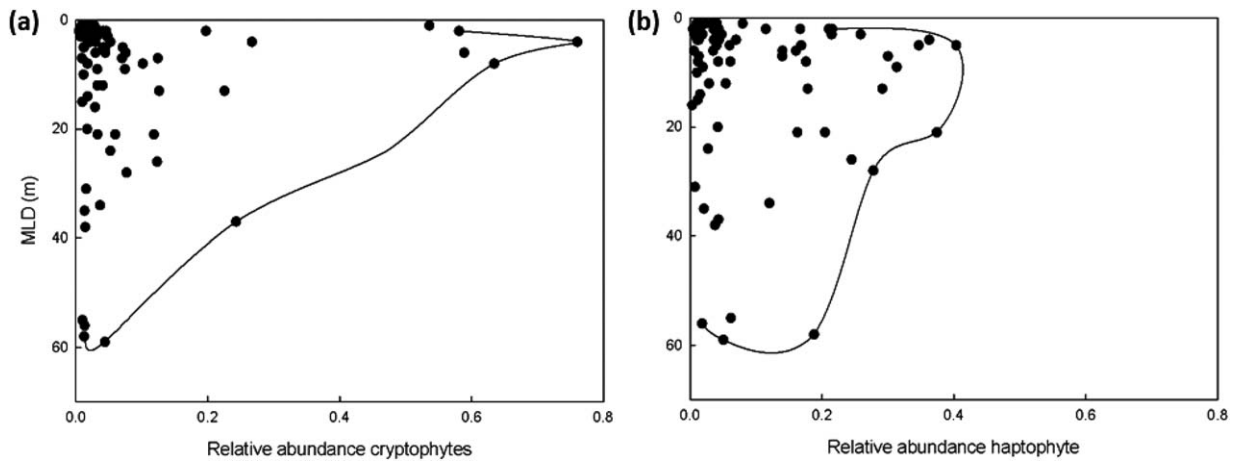


**Fig. 6.** Mixed layer depth (MLD) at the time of sampling plotted against the relative abundance of (a) cryptophytes or (b) haptophytes during the low biomass period (2007–2010). Cryptophytes preferred a relative shallow MLD while haptophytes were more diverse in their occurrence at variable MLDs. Convex hulls show the maximum relative abundance at various MLDs.

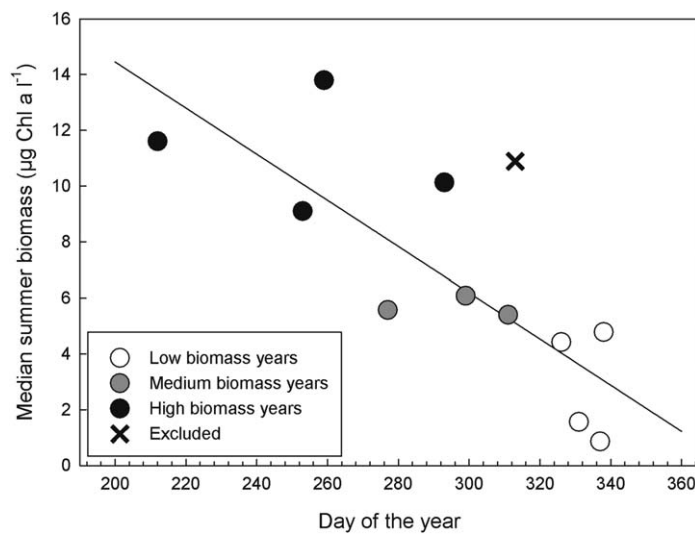


**Fig. 7.** Onset of summer melting in comparison to median summer biomass. The date of the salinity decrease is negatively correlated with median summer biomass ( $p = 0.002$ ;  $r^2 = 0.68$ ). The cross stands for a summer season for which no CTD data were collected for 1.5 months during the spring period. The colors indicate median summer concentrations of phytoplankton biomass (white: low, grey: medium and black: high).

concentrations are still higher than observed in open Southern Ocean (Bown et al. in press). In contrast, limitation by light (de Baar et al. 2005) or photoinhibition (Alderkamp et al. 2010) could not be excluded due to frequent changes in MLD and very high biomass concentrations (Venables et al. 2013). Yet none of these factors appeared to be limiting factors during the years of low biomass. Moreover, top down control on phytoplankton biomass cannot be excluded although it does not appear to govern phytoplankton growth rates in Ryder Bay (Venables et al. 2013). A shift

from grazers preying on large (by krill) to small phytoplankton (e.g., by ciliates or salps) could have an impact in low biomass years as small grazers can increase their numbers more rapidly than, for example, krill. Thus, small phytoplankton growth rates might be controlled more efficiently (Behrenfeld 2010). Also, while this paper focusses on 15 m Chl *a*, depth-integrated Chl *a* has been published previously and showed highly similar trends (Venables et al. 2013).

To assess the combination of our long term observations of the physical and biological conditions, we constructed a conceptual model. Analysis of the total number of winter fast-ice days revealed two clusters, high (89–124 days) and low (24–64 days) fast-ice winters, with a gap of 25 days separating the two clusters (Fig. 5a). Venables et al. (2013) suggested that this parameter is ultimately driving summer bloom magnitude. This grouping of years was used as a starting point for our conceptual model (Fig. 8). Summer stratification of the top 30 m was used as a second conditioner as diatoms, traditionally associated with high biomass, favor strong stratification (Table 2). Three different bins partitioned the summer into years of strong (283–264  $J m^{-2}$ ), intermediate (209–264  $J m^{-2}$ ) and weak (123–198  $J m^{-2}$ ) stratification. Finally, the years for which a full summer was covered were partitioned into three classes by median biomass based on the 15 years of Chl *a* measurements: high (9–14  $\mu g Chl a L^{-1}$ ), medium (5–7  $\mu g Chl a L^{-1}$ ), and low (0–5  $\mu g Chl a L^{-1}$ ). The minimum spanning tree in Fig. 5a further suggests that the low biomass conditions were a starting point at which the water column was still in a minimum, winter-like state. A more stable water column would improve the conditions for biomass growth to medium or higher levels. The grouping of high, medium and low biomass years suggests a strong dependence on the physical environment, further confirming the results from the correlation analyses (Table 2) and NPMANOVA (Table 1).



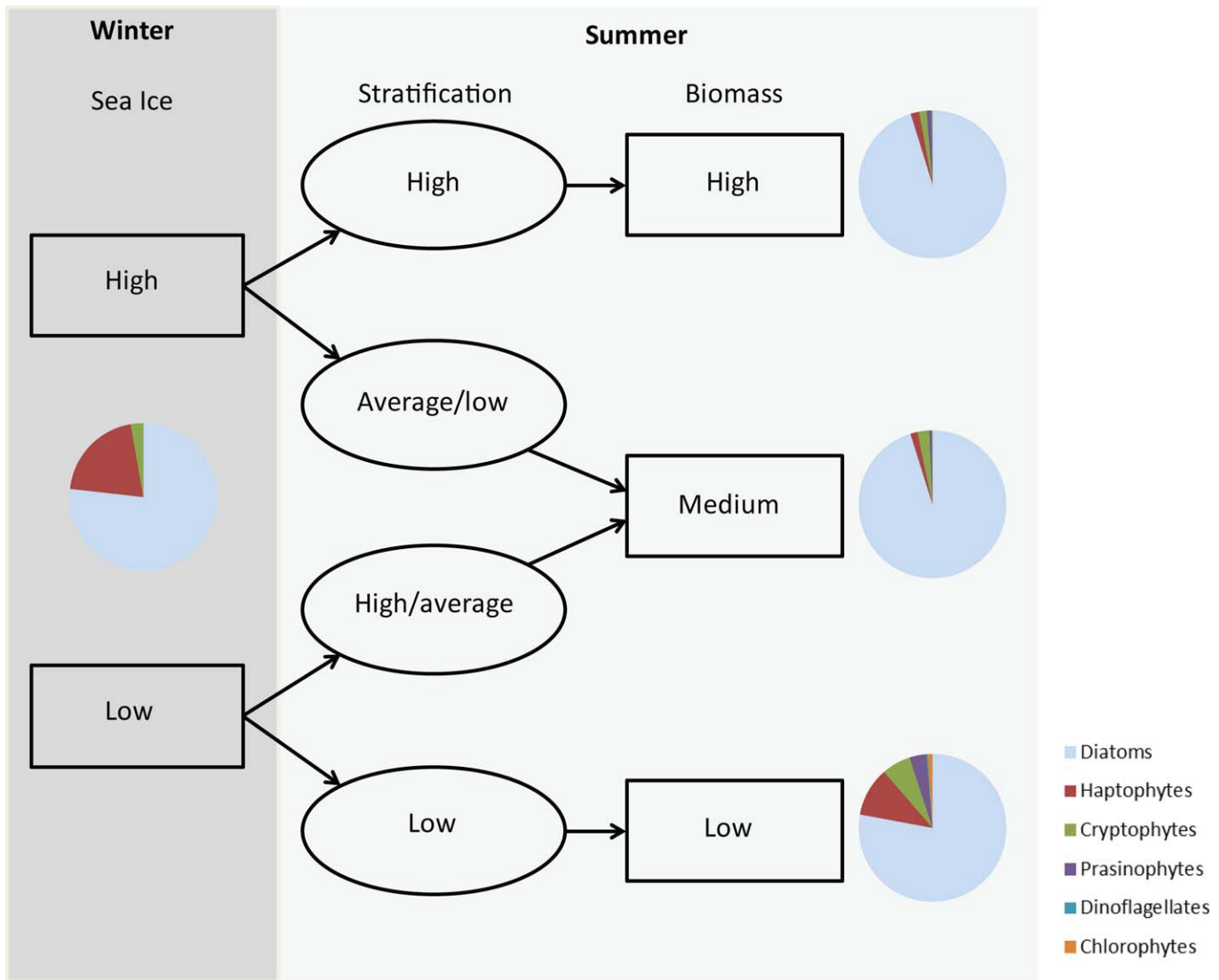


**Fig. 8.** Conceptual model linking the number of ice days to the strength of summer top 30m stratification. Two different sea ice modes (> 76 and < 76 days) can lead to three different stratification strength bins weak ( $283\text{--}264\text{ J m}^{-2}$ ), intermediate ( $209\text{--}264\text{ J m}^{-2}$ ), and weak ( $123\text{--}198\text{ J m}^{-2}$ ). Consequently, three classifications of median summer biomass (Chlorophyll *a* concentrations of 0–5, 5–7, and 9–14  $\mu\text{g Chl } a\text{ L}^{-1}$ ) allow the labeling of summers as low, medium or high biomass years. Also, median relative abundances for six phytoplankton groups during the winter and three summer classifications are shown.

Most years within our time series followed the classification by the model as proposed. The only exception was 1999–2000, where strength of summer stratification was intermediate while biomass was high ( $9.01\text{ }\mu\text{g Chl } a\text{ L}^{-1}$ ). The preceding winter MLD (mean 15.7 m) was much shallower than during any other winter in our time series, most likely due to a high number of fast ice days (114), thereby promoting exceptionally strong post-winter stratification and an early onset of phytoplankton growth. Also, at the end of November, Chl *a* concentrations were  $3.89\text{ }\mu\text{g L}^{-1}$  (Fig. 2a) while one week later it had increased to  $23.71\text{ }\mu\text{g } a\text{ L}^{-1}$ . This is the highest concentration observed in any of the 15 years of December observations apart from one sampling event on the 31 Dec 2010.

Our conceptual model identified three different categories of summers based on phytoplankton biomass. To understand how the phytoplankton community was composed within these categories, we pooled the years within the same category (Fig. 8). This resulted in three fingerprints showing that the high and medium biomass years were identical in their community composition. Cryptophytes, haptophytes and diatoms represented the bulk of the biomass, respectively 1.63%, 1.85%, and 95.22% for summers with high biomass and 2.59%, 1.56%, and 95.15% for medium biomass summers. Thus, there was little to no difference in relative contribution of the major groups between years categorized as high or medium summer biomass. However, low biomass years showed more cryptophytes (6.36%) and

haptophytes (10.72%) while the diatom fraction (77.90%) decreased. These last fractions were highly similar to those observed in winter. Thus, supporting our suggestion of summers preceded by winters with strong mixing may exhibit a persisting winter phytoplankton community.

We furthermore investigated if our conceptual model could explain the phytoplankton biomass and composition on the coastal WAP, mainly north of Marguerite Bay. The summertime phytoplankton community near Palmer station on Anvers Island experienced an increase of the relative contribution of cryptophytes related to event of increased melt water input (Moline et al. 2004; Saba et al. 2014). In contrast, in Marguerite Bay haptophytes and cryptophytes were seen to replace diatoms during low biomass years. Winter sea ice cover was low at Anvers Island and its duration shorter than in northern Marguerite Bay (Ducklow et al. 2013). Therefore, winters at Anvers island can be classified as low sea ice winters and, consequently, summer biomass can only reach low or medium values if following our conceptual model. A comparison of the Chl *a* measurements from Palmer Station sites B or E at Anvers Island and from RaTS revealed on average threefold higher Chl *a* at RaTS. The years in which the RaTS biomass approached that of Palmer Station were after winters with low ice cover, in agreement with our model. Also, the lack of winter sea ice and polynya-like properties of the northern WAP were likely to cause a deeper MLD during winter (Ducklow et al. 2013; Turner et al. 2013; Venables et al. 2013).

However, average summer MLD near Palmer station (1993–2012) was significantly shallower (~20 m) than in northern Marguerite Bay (~32 m; Ducklow et al. 2013). Thus, the deeper winter MLD and lower sea ice cover during spring suggests that meteoric water input, presumably predominantly of glacial origin, promotes stratification during summer and causes the shallow MLDs (Ducklow et al. 2013). We suspect low biomass summers can have elevated haptophytes, cryptophytes or a mixture thereof in agreement with satellite observations that suggest a decline in phytoplankton sizes (Montes-Hugo et al. 2009). To our knowledge, this study is the first to present high resolution, multi-year, year-round, and direct observations on how changes in size-class distribution and composition of the phytoplankton community at the coastal WAP relate to the changes in the physical environment. Earlier studies based on indirect satellite observations have estimated size-class distribution and/or total biomass over longer timespans (Montes-Hugo et al. 2008a, b, 2009).

Satellite derived biomass observations confirm our findings of declining summer phytoplankton biomass in the northern Marguerite Bay region (Fig. 2a in Montes-Hugo et al. 2009). This trend is dictated by two summers of extremely low biomass and decreased abundances of diatoms. While biomass at the southern WAP in the open ocean might be increasing (Montes-Hugo et al. 2009), coastal regions in the area do not follow this trend. Current trends of delayed sea ice formation

and strengthening wind are likely to cause deeper MLDs and weaker and later summer stratification (Meredith and King 2005; Montes-Hugo et al. 2009; Meredith et al. 2013). Even though there is a projected increase in glacial melt water which might add stability and thus partially counteract MLD deepening, oxygen isotope data at the RaTS site showed that this is not the dominant effect in determining changes in upper ocean stratification at this location (Meredith et al. 2013). Further delays in stratification onset due to the increasing winter MLD and lack of sea ice melt is likely to result in decreased productivity (Fig. 7). The deep mixing that causes unfavorable conditions for large diatom blooms is likely to become more frequent and the microphytoplankton fraction will most likely further decrease in abundance. We expect cryptophytes and (colonial forms of) *Phaeocystis* to be observed more frequently and become more important in the Antarctic ecosystem, in concert with declining phytoplankton biomass.

## Conclusions

Well-described trends over the northern WAP can now be projected further south as we connect our and previous observations into a conceptual model. Decreased (winter) sea ice cover will result in less abundant and smaller phytoplankton. We suggest that periods in the summer during low biomass years with a deeper MLD promote haptophytes (Arrigo et al. 1999). When MLDs become shallow, e.g., a shallow melt water lens of glacial origin on top of a relatively unstable water column, cryptophytes are likely to increase their presence (Moline et al. 2004; Mendes et al. 2013). A combination of these two mechanisms hold when compared to satellite observations that suggest a decline in phytoplankton sizes (Montes-Hugo et al. 2009). Our results nuances earlier suggestions of a cryptophytes dominated coastal WAP as haptophyte contributions were also observed to vary in relation to environmental changes (Saba et al. 2014).

Phytoplankton communities will have a different composition when current trends are projected forwards under global warming scenarios. Export of anthropogenic CO<sub>2</sub> by heavy diatoms might be diminished if the phytoplankton community will shift toward a flagellate-based systems (Weston et al. 2013). Further declines in krill and penguin stocks, as observed along the northern WAP, are likely to occur in Marguerite bay (Atkinson et al. 2008; Schofield et al. 2010; Constable et al. 2014; Saba et al. 2014), as diatom abundance declines. These projections will hold extensive consequences on the Antarctic ecosystem and biogeochemical cycling.

## References

- Alderkamp, A. C., H. J. W. de Baar, R. J. W. Visser, and K. R. Arrigo. 2010. Can photoinhibition control phytoplankton abundance in deeply mixed water columns of the Southern Ocean? *Limnol. Oceanogr.* **55**: 1248–1264. doi: 10.4319/lo.2010.55.3.1248

- Alderkamp, A. C., G. Kulk, A. G. J. Buma, R. J. W. Visser, G. L. van Dijken, M. M. Mills, and K. R. Arrigo. 2012a. The effect of iron limitation on the photophysiology of *Phaeocystis antarctica* (Prymnesiophyceae) and *Fragilariopsis cylindrus* (Bacillariophyceae) under dynamic irradiance. *J. Phycol.* **48**: 45–59. doi:[10.1111/j.1529-8817.2011.01098.x](https://doi.org/10.1111/j.1529-8817.2011.01098.x)
- Alderkamp, A. C., and others. 2012b. Iron from melting glaciers fuels phytoplankton blooms in the Amundsen Sea (Southern Ocean): Phytoplankton characteristics and productivity. *Deep. Res. Part II Top. Stud. Oceanogr.* **71-76**: 32–48. doi:[10.1016/j.dsr2.2012.03.005](https://doi.org/10.1016/j.dsr2.2012.03.005)
- Alderkamp, A. C., M. M. Mills, G. L. van Dijken, and K. R. Arrigo. 2013. Photoacclimation and non-photochemical quenching under in situ irradiance in natural phytoplankton assemblages from the Amundsen Sea, Antarctica. *Mar. Ecol. Prog. Ser.* **475**: 15–34. doi:[10.3354/meps10097](https://doi.org/10.3354/meps10097)
- Anderson, M. J. 2001. A new method for non-parametric multivariate analysis of variance. *Austral Ecol.* **26**: 32–46. doi:[10.1111/j.1442-9993.2001.tb00081.x](https://doi.org/10.1111/j.1442-9993.2001.tb00081.x)
- Annett, A. L., D. S. Carson, X. Crosta, A. Clarke, and R. S. Ganeshram. 2010. Seasonal progression of diatom assemblages in surface waters of Ryder Bay, Antarctica. *Polar Biol.* **33**: 13–29. doi:[10.1007/s00300-009-0681-7](https://doi.org/10.1007/s00300-009-0681-7)
- Annett, A. L., M. Skiba, S. F. Henley, H. J. Venables, M. P. Meredith, P. J. Statham, and R. S. Ganeshram. 2015. Comparative roles of upwelling and glacial iron sources in Ryder Bay, coastal western Antarctic Peninsula. *Mar. Chem.* **176**: 21–33. doi:[10.1016/j.marchem.2015.06.017](https://doi.org/10.1016/j.marchem.2015.06.017)
- Arrigo, K. R., D. H. Robinson, D. L. Worthen, R. B. Dunbar, G. R. DiTullio, M. VanWoert, and M. P. Lizotte. 1999. Phytoplankton community structure and the drawdown of nutrients and CO<sub>2</sub> in the Southern Ocean. *Science* (80-). **283**: 365–367. doi:[10.1126/science.283.5400.365](https://doi.org/10.1126/science.283.5400.365)
- Atkinson, A., V. Siegel, E. Pakhomov, and P. Rothery. 2004. Long-term decline in krill stock and increase in salps within the Southern Ocean. *Nature.* **432**: 100–103. doi:[10.1038/nature02996](https://doi.org/10.1038/nature02996)
- Atkinson, A., and others. 2008. Oceanic circumpolar habitats of Antarctic krill. *Mar. Ecol. Prog. Ser.* **362**: 1–23. doi:[10.3354/meps07498](https://doi.org/10.3354/meps07498)
- Behrenfeld, M. J. 2010. Abandoning Sverdrup's critical depth hypothesis on phytoplankton blooms critical depth hypothesis abandoning Sverdrup's on phytoplankton. *Ecology* **91**: 977–989. doi:[10.1890/09-1207.1](https://doi.org/10.1890/09-1207.1)
- Bown, J., P. Laan, S. Ossebaar, K. Bakker, P. D. Rozema, and H. J. W. de Baar. 2006. Bioactive trace metal time series during Austral summer in Ryder Bay, Western Antarctic Peninsula. *Deep Sea Res. Part II Top. Stud. Oceanogr.* doi:[10.1016/j.dsr2.2016.07.004](https://doi.org/10.1016/j.dsr2.2016.07.004)
- Buma, A. G. J., W. W. C. Gieskes, and H. A. Thomsen. 1992. Abundance of cryptophyceae and chlorophyll b-containing organisms in the Weddell-Scotia Confluence area in the spring of 1988. *Polar Biol.* **12**: 43–52. doi:[10.1007/BF00239964](https://doi.org/10.1007/BF00239964)
- Clarke, A., M. P. Meredith, M. I. Wallace, M. A. Brandon, and D. N. Thomas. 2008. Seasonal and interannual variability in temperature, chlorophyll and macronutrients in northern Marguerite Bay, Antarctica. *Deep. Res. Part II Top. Stud. Oceanogr.* **55**: 1988–2006. doi:[10.1016/j.dsr2.2008.04.035](https://doi.org/10.1016/j.dsr2.2008.04.035)
- Constable, A. J., and others. 2014. Climate change and southern ocean ecosystems I: How changes in physical habitats directly affect marine biota. *Glob. Chang. Biol.* 3004–3025. doi:[10.1111/gcb.12623](https://doi.org/10.1111/gcb.12623)
- Cook, A. J., A. J. Fox, D. G. Vaughan, and J. G. Ferrigno. 2005. Retreating glacier fronts on the Antarctic Peninsula over the past half-century. *Science* **308**: 541–544. doi:[10.1126/science.1104235](https://doi.org/10.1126/science.1104235)
- de Baar, H. J. W., and others. 2005. Synthesis of iron fertilization experiments: From the iron age in the age of enlightenment. *J. Geophys. Res. - Ocean.* **110**: 1–24. doi:[10.1029/2004JC002601](https://doi.org/10.1029/2004JC002601)
- Depoorter, M. A., J. L. Bamber, J. A. Griggs, J. T. M. Lenaerts, S. R. M. Ligtenberg, M. R. van den Broeke, and G. Moholdt. 2013. Calving fluxes and basal melt rates of Antarctic ice shelves. *Nature* **502**: 89–92. doi:[10.1038/nature12567](https://doi.org/10.1038/nature12567)
- Ducklow, H. W., and others. 2013. West Antarctic Peninsula: An ice-dependent coastal marine ecosystem in transition. *Oceanography* **26**: 190–203. doi:[10.5670/oceanog.2013.62](https://doi.org/10.5670/oceanog.2013.62)
- Flores, H., and others. 2012. Impact of climate change on Antarctic krill. *Mar. Ecol. Prog. Ser.* **458**: 1–19. doi:[10.3354/meps09831](https://doi.org/10.3354/meps09831)
- Garibotti, I. A., M. Vernet, W. A. Kozlowski, and M. E. Ferrario. 2003. Composition and biomass of phytoplankton assemblages in coastal Antarctic waters: A comparison of chemotaxonomic and microscopic analyses. *Mar. Ecol. Prog. Ser.* **247**: 27–42. doi:[10.3354/meps247027](https://doi.org/10.3354/meps247027)
- Garibotti, I. A., M. Vernet, and M. E. Ferrario. 2005. Annually recurrent phytoplanktonic assemblages during summer in the seasonal ice zone west of the Antarctic Peninsula (Southern Ocean). *Deep. Res. Part I Oceanogr. Res. Pap.* **52**: 1823–1841. doi:[10.1016/j.dsr.2005.05.003](https://doi.org/10.1016/j.dsr.2005.05.003)
- Hammer, Ø., D. A. T. Harper, and P. D. Ryan. 2001. PAST: Palaeontological statistics software package for education and data analysis. *Palaeontol. Electron.* **4**: 1–9. doi:[10.1163/001121611X5666785](https://doi.org/10.1163/001121611X5666785)
- Harangozo, S. A. 2006. Atmospheric circulation impacts on winter maximum sea ice extent in the west Antarctic Peninsula region (1979-2001). *Geophys. Res. Lett.* **33**: L02502. doi:[10.1029/2005GL024978](https://doi.org/10.1029/2005GL024978)
- Higgins, H. H. W., S. W. Wright, L. Schlüter, and L. Schlüter. 2012. Quantitative interpretation of chemotaxonomic pigment data, 257–313 *In* S. Roy, C.A. Llewellyn, E.S. Egeland, and G. Johnsen [eds.], *Phytoplankton pigments: Characterization, chemotaxonomy and applications in oceanography*. Cambridge University Press.

- Holm, S. 1979. A simple sequentially rejective multiple test procedure. *Scand. J. Stat.* **6**: 65–70. doi:[10.2307/4615733](https://doi.org/10.2307/4615733)
- Kozłowski, W. A., D. Deutschman, I. Garibotti, C. Trees, and M. Vernet. 2011. An evaluation of the application of CHEMTAX to Antarctic coastal pigment data. *Deep. Res. Part I Oceanogr. Res. Pap.* **58**: 350–364. doi:[10.1016/j.dsr.2011.01.008](https://doi.org/10.1016/j.dsr.2011.01.008)
- Kropuenske, L. R., M. M. Mills, G. L. van Dijken, S. Bailey, D. H. Robinson, N. A. Welschmeyer, and K. R. Arrigo. 2009. Photophysiology in two major Southern Ocean phytoplankton taxa: Photoprotection in *Phaeocystis antarctica* and *Fragilariopsis cylindrus*. *Limnol. Oceanogr.* **54**: 1176–1196. doi:[10.4319/lo.2009.54.4.1176](https://doi.org/10.4319/lo.2009.54.4.1176)
- Latasa, M., R. Scharek, M. Vidal, G. Vila-Reixach, A. Gutiérrez-Rodríguez, M. Emelianov, and J. M. Gasol. 2010. Preferences of phytoplankton groups for waters of different trophic status in the northwestern Mediterranean sea. *Mar. Ecol. Prog. Ser.* **407**: 27–42. doi:[10.3354/meps08559](https://doi.org/10.3354/meps08559)
- Mackey, M. D., D. J. Mackey, H. W. Higgins, and S. W. Wright. 1996. CHEMTAX - A program for estimating class abundances from chemical markers: Application to HPLC measurements of phytoplankton. *Mar. Ecol. Prog. Ser.* **144**: 265–283. doi:[10.3354/meps144265](https://doi.org/10.3354/meps144265)
- Mendes, C. R. B., M. S. de Souza, V. M. T. Garcia, M. C. Leal, V. Brotas, and C. A. E. Garcia. 2012. Dynamics of phytoplankton communities during late summer around the tip of the Antarctic Peninsula. *Deep. Res. Part I Oceanogr. Res. Pap.* **65**: 1–14. doi:[10.1016/j.dsr.2012.03.002](https://doi.org/10.1016/j.dsr.2012.03.002)
- Mendes, C. R. B., V. M. Tavano, M. C. Leal, M. S. de Souza, V. Brotas, and C. A. E. Garcia. 2013. Shifts in the dominance between diatoms and cryptophytes during three late summers in the Bransfield Strait (Antarctic Peninsula). *Polar Biol.* **36**: 537–547. doi:[10.1007/s00300-012-1282-4](https://doi.org/10.1007/s00300-012-1282-4)
- Meredith, M. P., I. A. Renfrew, A. Clarke, J. C. King, and M. A. Brandon. 2004. Impact of the 1997/98 ENSO on upper ocean characteristics in Marguerite Bay, western Antarctic Peninsula. *J. Geophys. Res. C Ocean.* **109**: 1–19. doi:[10.1029/2003JC001784](https://doi.org/10.1029/2003JC001784)
- Meredith, M. P., and J. C. King. 2005. Rapid climate change in the ocean west of the Antarctic Peninsula during the second half of the 20th century. *Geophys. Res. Lett.* **32**: 1–5. doi:[10.1029/2005GL024042](https://doi.org/10.1029/2005GL024042)
- Meredith, M. P., M. A. Brandon, M. I. Wallace, A. Clarke, M. J. Leng, I. A. Renfrew, N. P. M. van Lipzig, and J. C. King. 2008. Variability in the freshwater balance of northern Marguerite Bay, Antarctic Peninsula: Results from delta O-18. *Deep. Res. Part II Top. Stud. Oceanogr.* **55**: 309–322. doi:[10.1016/j.dsr2.2007.11.005](https://doi.org/10.1016/j.dsr2.2007.11.005)
- Meredith, M. P., H. J. Venables, A. Clarke, H. W. Ducklow, M. Erickson, M. J. Leng, J. T. M. M. Lenaerts, and M. R. van den Broeke. 2010. Changes in the freshwater composition of the upper ocean west of the Antarctic Peninsula during the first decade of the 21st century. *Prog. Oceanogr.* **87**: 127–143. doi:[10.1016/j.pocean.2010.09.019](https://doi.org/10.1016/j.pocean.2010.09.019)
- Meredith, M. P., and others. 2013. The freshwater system west of the Antarctic Peninsula: spatial and temporal changes. *J. Clim.* **26**: 1669–1684. doi:[10.1175/JCLI-D-12-00246.1](https://doi.org/10.1175/JCLI-D-12-00246.1)
- Moline, M. A., H. Claustre, T. K. Frazer, O. Schofield, and M. Vernet. 2004. Alteration of the food web along the Antarctic Peninsula in response to a regional warming trend. *Glob. Chang. Biol.* **10**: 1973–1980. doi:[10.1111/j.1365-2486.2004.00825.x](https://doi.org/10.1111/j.1365-2486.2004.00825.x)
- Montes-Hugo, M. A., M. Vernet, D. Martinson, R. Smith, and R. Iannuzzi. 2008a. Variability on phytoplankton size structure in the western Antarctic Peninsula (1997–2006). *Deep. Res. Part II Top. Stud. Oceanogr.* **55**: 2106–2117. doi:[10.1016/j.dsr2.2008.04.036](https://doi.org/10.1016/j.dsr2.2008.04.036)
- Montes-Hugo, M. A., M. Vernet, R. Smith, and K. Carder. 2008b. Phytoplankton size-structure on the western shelf of the Antarctic Peninsula: A remote-sensing approach. *Int. J. Remote Sens.* **29**: 801–829. doi:[10.1080/01431160701297615](https://doi.org/10.1080/01431160701297615)
- Montes-Hugo, M., S. C. Doney, H. W. Ducklow, W. R. Fraser, D. Martinson, S. E. Stammerjohn, and O. Schofield. 2009. Recent changes in phytoplankton communities associated with rapid regional climate change along the western Antarctic Peninsula. *Science* **323**: 1470–1473. doi:[10.1126/science.1164533](https://doi.org/10.1126/science.1164533)
- Perl, J. 2009. The SDU (CHORS) Method, p. 89–91. *In* The Third SeaWiFS HPLC Analysis Round-Robin Experiment (SeaHARRE-3), NASA.
- Piquet, A. M. T., H. Bolhuis, M. P. Meredith, and A. G. J. Buma. 2011. Shifts in coastal Antarctic marine microbial communities during and after melt water-related surface stratification. *FEMS Microbiol. Ecol.* **76**: 413–427. doi:[10.1111/j.1574-6941.2011.01062.x](https://doi.org/10.1111/j.1574-6941.2011.01062.x)
- Reiss, C., J. Walsh, and M. Goebel. 2015. Winter preconditioning determines feeding ecology of *Euphausia superba* in the Antarctic Peninsula. *Mar. Ecol. Prog. Ser.* **519**: 89–101. doi:[10.3354/meps11082](https://doi.org/10.3354/meps11082)
- Rignot, E., S. Jacobs, J. Mouginot, and B. Scheuchl. 2013. Ice-shelf melting around Antarctica. *Science* **341**: 266–270. doi:[10.1126/science.1235798](https://doi.org/10.1126/science.1235798)
- Saba, G. K., and others. 2014. Winter and spring controls on the summer food web of the coastal West Antarctic Peninsula. *Nat. Commun.* **5**: 4318. doi:[10.1038/ncomms5318](https://doi.org/10.1038/ncomms5318)
- Schofield, O., H. W. Ducklow, D. G. Martinson, M. P. Meredith, M. A. Moline, and W. R. Fraser. 2010. How do polar marine ecosystems respond to rapid climate change? *Science* **328**: 1520–1523. doi:[10.1126/science.1185779](https://doi.org/10.1126/science.1185779)
- Simpson, J. H., C. M. Allen, and N. C. G. Morris. 1978. Fronts on the continental shelf. *J. Geophys. Res.* **83**: 4607. doi:[10.1029/JC083iC09p04607](https://doi.org/10.1029/JC083iC09p04607)
- Smith, R. C., and S. E. Stammerjohn. 2001. Variations of surface air temperature and sea-ice extent in the western Antarctic Peninsula region. *Ann. Glaciol.* **33**: 493–500. doi:[10.3189/172756401781818662](https://doi.org/10.3189/172756401781818662)
- Stammerjohn, S. E., D. G. Martinson, R. C. Smith, and R. A. Iannuzzi. 2008a. Sea ice in the western Antarctic



- Peninsula region: Spatio-temporal variability from ecological and climate change perspectives. *Deep. Res. Part II Top. Stud. Oceanogr.* **55**: 2041–2058. doi:[10.1016/j.dsr2.2008.04.026](https://doi.org/10.1016/j.dsr2.2008.04.026)
- Stammerjohn, S. E., D. G. Martinson, R. C. Smith, X. Yuan, and D. Rind. 2008b. Trends in Antarctic annual sea ice retreat and advance and their relation to El Niño–Southern Oscillation and Southern Annular Mode variability. *J. Geophys. Res.* **113**: 20. doi:[10.1029/2007JC004269](https://doi.org/10.1029/2007JC004269)
- Steinberg, D. K., and others. 2015. Long-term (1993–2013) changes in macrozooplankton off the Western Antarctic Peninsula. *Deep. Res. Part I Oceanogr. Res. Pap.* **101**: 54–70. doi:[10.1016/j.dsr.2015.02.009](https://doi.org/10.1016/j.dsr.2015.02.009)
- Sverdrup, H. 1953. On conditions for the vernal blooming of phytoplankton. *J. Du Cons.* **18**: 287–295. doi:[10.4319/lom.2007.5.269](https://doi.org/10.4319/lom.2007.5.269)
- Trivelpiece, W. Z., J. T. Hinke, A. K. Miller, C. S. Reiss, S. G. Trivelpiece, and G. M. Watters. 2011. Variability in krill biomass links harvesting and climate warming to penguin population changes in Antarctica. *Proc. Natl. Acad. Sci. USA* **108**: 7625–7628. doi:[10.1073/pnas.1016560108](https://doi.org/10.1073/pnas.1016560108)
- Turner, J., and others. 2005. Antarctic climate change during the last 50 years. *Int. J. Climatol.* **25**: 279–294. doi:[10.1002/joc.1130](https://doi.org/10.1002/joc.1130)
- Turner, J., T. Maksym, T. Phillips, G. J. Marshall, and M. P. Meredith. 2013. The impact of changes in sea ice advance on the large winter warming on the western Antarctic Peninsula. *Int. J. Climatol.* **33**: 852–861. doi:[10.1002/joc.3474](https://doi.org/10.1002/joc.3474)
- van de Poll, W. H., P. J. Janknegt, M. A. van Leeuwe, R. J. W. Visser, and A. G. J. Buma. 2009. Excessive irradiance and antioxidant responses of an Antarctic marine diatom exposed to iron limitation and to dynamic irradiance. *J. Photochem. Photobiol. B Biol.* **94**: 32–37. doi:[10.1016/j.jphotobiol.2008.09.003](https://doi.org/10.1016/j.jphotobiol.2008.09.003)
- van Heukelem, L., and C. S. Thomas. 2001. Computer-assisted high-performance liquid chromatography method development with applications to the isolation and analysis of phytoplankton pigments. *J. Chromatogr. A* **910**: 31–49. doi:[10.1016/S0378-4347\(00\)00603-4](https://doi.org/10.1016/S0378-4347(00)00603-4)
- van Leeuwe, M. A., L. A. Villerius, J. Roggeveld, R. J. W. Visser, and J. Stefels. 2006. An optimized method for automated analysis of algal pigments by HPLC. *Mar. Chem.* **102**: 267–275. doi:[10.1016/j.marchem.2006.05.003](https://doi.org/10.1016/j.marchem.2006.05.003)
- van Leeuwe, M. A., R. J. W. Visser, and J. Stefels. 2014. The pigment composition of *Phaeocystis antarctica* (Haptophyceae) under various conditions of light, temperature, salinity, and iron. *J. Phycol.* **50**: 1070–1080. doi:[10.1111/jpy.12238](https://doi.org/10.1111/jpy.12238)
- Vaughan, D. G., and others. 2003. Recent rapid regional climate warming on the Antarctic Peninsula. *Clim. Change.* **60**: 243–274. doi:[10.1023/A:1026021217991](https://doi.org/10.1023/A:1026021217991)
- Venables, H. J., A. Clarke, and M. P. Meredith. 2013. Winter-time controls on summer stratification and productivity at the western Antarctic Peninsula. *Limnol. Oceanogr.* **58**: 1035–1047. doi:[10.4319/lo.2013.58.3.1035](https://doi.org/10.4319/lo.2013.58.3.1035)
- Venables, H. J., and M. P. Meredith. 2014. Feedbacks between ice cover, ocean stratification, and heat content in Ryder Bay, western Antarctic Peninsula. *J. Geophys. Res. Ocean.* **119**: 5323–5336. doi:[10.1002/jgrc.20224](https://doi.org/10.1002/jgrc.20224)
- Weston, K., and others. 2013. Primary production export flux in Marguerite Bay (Antarctic Peninsula): Linking upper water-column production to sediment trap flux. *Deep. Res. Part I Oceanogr. Res. Pap.* **75**: 52–66. doi:[10.1016/j.dsr.2013.02.001](https://doi.org/10.1016/j.dsr.2013.02.001)
- Wood, L. W. 1985. Chloroform–methanol extraction of chlorophyll. *A. Can. J. Fish. Aquat. Sci.* **42**: 38–43. doi:[10.1139/f85-005](https://doi.org/10.1139/f85-005)
- Wright, S. W., A. Ishikawa, H. J. Marchant, A. T. Davidson, R. L. van den Eenden, and G. V. Nash. 2009. Composition and significance of picophytoplankton in Antarctic waters. *Polar Biol.* **32**: 797–808. doi:[10.1007/s00300-009-0582-9](https://doi.org/10.1007/s00300-009-0582-9)
- Wright, S. W., R. L. van den Eenden, I. Pearce, A. T. Davidson, F. J. Scott, and K. J. Westwood. 2010. Phytoplankton community structure and stocks in the Southern Ocean (30–80°E) determined by CHEMTAX analysis of HPLC pigment signatures. *Deep. Res. Part II Top. Stud. Oceanogr.* **57**: 758–778. doi:[10.1016/j.dsr2.2009.06.015](https://doi.org/10.1016/j.dsr2.2009.06.015)

### Acknowledgments

We thank all the Marine Assistants and other staff at Rothera and in Cambridge who have contributed to the collection of the samples and data used here. Also, we thank Ronald Visser, who assisted with HPLC measurements and Simon Wright for providing an original version of CHEMTAX. Gemma Kulk and two anonymous reviewers are thanked for valuable discussions. This research was funded by the Netherlands Polar Programme (866.10.105). RaTS is funded by the Natural Environment Research Council, and is a component of the BAS Polar Oceans programme.

### Conflict of Interest

None declared.

Submitted 16 March 2016

Revised 20 June 2016

Accepted 19 July 2016

Associate editor: Susanne Menden-Deuer